Journal of Magnetism and Magnetic Materials 474 (2019) 343–346

Contents lists available at ScienceDirect

Journal of Magnetism and Magnetic Materials

journal homepage: www.elsevier.com/locate/jmmm

Research articles

Room-temperature magnetic Heusler compound $Fe_2Ti_{0.5}Co_{0.5}Si$ with semiconducting behavior

Yunlong Jin[a,b,1,*], Yi Yang[a,1], Shah Valloppilly[b], Sy-Hwang Liou[a,b], David J. Sellmyer[a,b]

[a] Department of Physics and Astronomy, University of Nebraska, Lincoln, NE 68588, United States
[b] Nebraska Center for Materials and Nanoscience, University of Nebraska, Lincoln, NE 68588, United States

ARTICLE INFO

Keywords:
Magnetic semiconducting behavior
Heusler compound
High Curie temperature

ABSTRACT

The structural, magnetic and electron-transport properties of $Fe_2Ti_{0.5}Co_{0.5}Si$ are investigated. It is demonstrated that rapidly quenched $Fe_2Ti_{0.5}Co_{0.5}Si$ ribbons crystallize in the $L2_1$ structure, indicating a full Heusler compound, and exhibit ferromagnetism with a high Curie temperature of about 790 K. Moreover, $Fe_2Ti_{0.5}Co_{0.5}Si$ exhibits semiconducting behavior with a negative temperature coefficient of resistivity, a room-temperature resistivity of about 6.5 mΩ cm and a residual resistivity ρ_0 of about 6.75 mΩ cm. The carrier concentration n is 1.15×10^{20} cm^{-3} at 5 K. The magnetic semiconducting behavior with a high Curie temperature makes this material promising for room-temperature spintronic and magnetic applications.

1. Introduction

Spintronics aims to develop devices that exploit electronic spins for manipulation, storage and retrieval of data, replacing the conventional charge-based devices [1,2]. In spintronic devices, spin injection, i.e., efficient generation of a spin-polarized current, is an essential issue [3]. Half-metallic ferromagnets [4] and dilute magnetic semiconductors (DMS) [5,6], have attracted much attention because these materials, in principle, can produce completely (100%) spin-polarized currents. In addition, a high Curie temperature (T_C), i.e., well above room temperature (RT), is required for device applications, although it is elusive, particularly in certain dilute magnetic semiconductors such as (Ga, X)Y, (X = Mn, Co, Fe, Ni), (Y = As, N) [6]. In recent years, there has been an upsurge of research on new materials with these desired properties, especially the family of Heusler compounds. Many half-Heusler compounds ($C1_b$ structure) are found to be nonmagnetic semiconducting materials [7–9]. However, only a small number of full-Heusler compounds ($L2_1$ structure) are found to be semiconductors [10]. Among the rare full-Heusler semiconductors, Fe_2TiSi has been calculated to be a n-type semiconducting material, with a sizeable gap (0.41 eV) and large Seebeck coefficient (−300 μV/K at room temperature) [11]. Based on the Slater-Pauling rule, Fe_2TiSi (24 valence electrons) is predicted to possess a magnetic moment of 0 μ_B/f.u. [12]. Accordingly, single-phase metastable Fe_2TiSi has been synthesized as a paramagnetic semiconducting material with a band gap of about 0.4 eV, exhibiting an extremely weak magnetization and a Kondo-like effect at low temperature [13]. Fe_2TiSn is found to be a semimetal [14,15], although also predicted to be a semiconductor [11]. On the other hand, the Heusler compound Fe_2CoSi (29 valence electrons) is known as a ferromagnetic material with a quite high T_C of 1038 K and magnetization of 4.92 μ_B/f.u. at 5 K. DFT calculations show a zero-gap half-metallic valence-band spectrum close to the Fermi energy [16]. In order to combine the high saturation magnetization of Fe_2CoSi with the semiconducting property of Fe_2TiSi, it is of interest to replace half of the Ti atoms in the compound Fe_2TiSi with Co atoms. In this paper, we demonstrate the synthesis of ferromagnetic semiconducting $Fe_2Ti_{0.5}Co_{0.5}Si$ (26.5 valence electrons), and the structural, magnetic and transport properties are measured and discussed.

2. Materials and methods

High-purity elements were made into ingots of $Fe_2Ti_{0.5}Co_{0.5}Si$ by arc melting in an argon atmosphere. Ingots were melted and ejected in a melt spinner from a quartz tube onto the surface of a copper wheel rotating at a speed of 25 m/s. This rapid quenching technique produced ribbon samples, about 2 mm wide and 50 μm thick. The investigation of the crystal structures in the samples was performed using powder X-ray diffraction (XRD) in a PANalytical Empyrean diffractometer with copper Kα radiation (wavelength of 1.5406 Å), and the confirmation of elemental compositions was done with energy-dispersive X-ray

* Corresponding author.
E-mail address: yunlongjin@huskers.unl.edu (Y. Jin).
[1] The authors contributed equally.

https://doi.org/10.1016/j.jmmm.2018.11.063
Received 21 August 2018; Received in revised form 20 October 2018; Accepted 8 November 2018
Available online 09 November 2018
0304-8853/

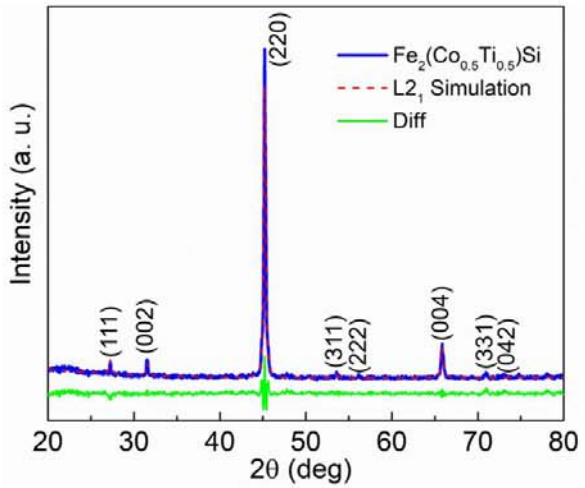

Fig. 1. Powder XRD pattern of the $Fe_2Ti_{0.5}Co_{0.5}Si$ compound prepared by melt spinning (blue) and the pattern simulated for the $L2_1$ structure of the $Fe_2Ti_{0.5}Co_{0.5}Si$ compound (dash on red). (For interpretation of the references to color in this figure legend, the reader is referred to the web version of this article.)

spectroscopy (EDX) in a FEI Nova NanoSEM450. Magnetic properties and electron-transport properties were measured with a Quantum Design VersaLab magnetometer and Physical Properties Measurement System (PPMS). In the measurement of magnetization, the applied magnetic field was parallel to the length of the ribbons, whereas the magnetoresistance and Hall measurements were done with the magnetic field perpendicular to the ribbons.

3. Results and discussion

3.1. XRD analysis

Fig. 1 shows the powder XRD pattern of $Fe_2Ti_{0.5}Co_{0.5}Si$, which contains the fundamental (1 1 1) and (0 0 2) superlattice peaks at 27° and 32° respectively, indicating the $L2_1$ structure. In order to understand the crystalline order (B2, $L2_1$), long-range order parameters S_{L21} and S_{B2} can be used as a measure of closeness to ideal $L2_1$ and B2 structures with the equations: $S_{B2}^2 = I_{200} \cdot I_{400}^{fullorder} / I_{400} \cdot I_{200}^{fullorder}$ and $(S_{L21}(3 - S_{B2})/2)^2 = I_{111} \cdot I_{220}^{fullorder} / I_{220} \cdot I_{111}^{fullorder}$, where I_{hkl} and $I_{hkl}^{fullorder}$ are respectively the experimental diffraction intensities for the (h k l) planes and the reference intensities calculated for the fully ordered alloys. The value of S_{L21} was calculated to be 97% based on the intensities of the corresponding peaks in the XRD pattern of the powder sample prepared with the as-quenched ribbons. In order to confirm the calculated S_{L21}, a Rietveld analysis of the XRD pattern was performed and is as shown in Fig. 1 (red dashed line). The value of S_{L21} from the Rietveld analysis is in very good agreement with the above value, which suggests that the $Fe_2Ti_{0.5}Co_{0.5}Si$ ribbons have mainly the ordered $L2_1$ structure with little disorder. $L2_1$-type structure formation also has been predicted theoretically in most of the Ti-based full Heusler compounds [17]. However, X-ray diffraction analysis confirms that the stoichiometry and the site occupancy are different in our samples compared with those Ti-based full Heusler compounds. The elemental compositions determined by EDX analysis are very close (within 5%) to the values estimated with the initial weight of the constituent elements.

3.2. Magnetism

Fig. 2(a) shows isothermal magnetization M(H) curves of the $Fe_2Ti_{0.5}Co_{0.5}Si$ Heusler compound measured at 5 K and 300 K. The M (H) loops exhibit ferromagnetism with small coercivities of about 50 Oe at both 5 K and 300 K. The magnetization of the $Fe_2Ti_{0.5}Co_{0.5}Si$ ribbons is 480 emu/cm^3 (2.36 μ_B/f.u.) at 5 K and 450 emu/cm^3 (2.21 μ_B/f.u.) at 300 K, which is contrary to the very weak magnetism in Fe_2TiSi and Fe_2VAl [10,13,18–20], but lower than that of Fe_2CoSi [16]. Compared with the theoretical value of 2.5 μ_B/f.u., predicted by Slater-Pauling rule [12], the magnetization is slightly lower possibly due to the minor chemical disorder. Fig. 2(b) shows the temperature dependence of the magnetization M(T) of the $Fe_2Ti_{0.5}Co_{0.5}Si$ compound measured under a magnetic field of 10 kOe. The Curie temperature is about 790 K, much higher than that of diluted magnetic semiconductors (Ga, X)Y, (X = Mn, Co, Fe, Ni), (Y = As, N) [6]. The partial substitution of Ti by Co produces enhanced magnetic properties in the compound.

3.3. Electron transport

The temperature dependence of the longitudinal resistivity ρ_{xx} was measured between 5 K and 300 K and the magnetoresistance (MR) was measured at various temperatures with a maximum applied magnetic field of 70 kOe. As shown in Fig. 3(a), the resistivity ρ_{xx} exhibits a negative temperature coefficient, indicating semiconducting behavior in the $Fe_2Ti_{0.5}Co_{0.5}Si$ compound. The residual resistivity ρ_0 in this material is about 6.75 mΩ cm, which is at least one order higher than the values in metallic Heusler compounds Fe_2CoSi [16] and Co_2TiSi [21] and in spin-gapless semiconducting Heusler compounds Mn_2CoAl [22,23] and CoFeMnSi [24,25]. As reported for the paramagnetic semiconducting Fe_2TiSi films, the band gap is about 0.4 eV and the resistivity shows a little change in a wide temperature range [13]. Compared to Fe_2TiSi, $Fe_2Ti_{0.5}Co_{0.5}Si$ has a similar resistivity but the conductivity of this material is more complicated. The resistivity of $Fe_2Ti_{0.5}Co_{0.5}Si$ does not show a significant change between 5 K and 300 K possibly due to a smaller band gap than that of a usual semiconductor. It may even be close to the case of spin-gapless semiconductors that have zero band gap and nearly temperature-independent conductivities [22–24], in consideration of the magnetoresistance and carrier concentration to be discussed in the remaining of this paper. The variation in the overall temperature dependence of resistivity is similar to extrinsic to intrinsic transitions in semiconductors such as CoFeMnSi [25] and ZrSTe [26]. Moreover, at temperatures lower than 100 K, the inset shows an essentially logarithmic temperature dependence, quite similar to the temperature-dependent behavior of the Kondo effect [13,27–30]. Fig. 3(b) shows the transverse magnetoresistance of the $Fe_2Ti_{0.5}Co_{0.5}Si$ compound. The low-field MR has a negative slope at all temperatures from zero field to the saturation field of magnetization and is attributed to the anisotropic magnetoresistance (AMR). After the saturation of magnetization, the change of the slope from being negative to being positive as the temperature increases is uncommon in traditional magnetic materials. However, similar phenomena are reported in various Heusler compounds such as Fe_2CoSi, CoFeCrAl and the bulk spin-gapless semiconductor Mn_2CoAl [16,23,31]. The negative MR at low temperatures under high magnetic fields is consistent with spin-dependent scattering of conduction electrons, while the positive MR at the room temperature may be attributed to the ordinary Lorentz-force mechanism. Two mechanisms of MR have different temperature dependences, thus competing with each other as the temperature increases. The MR is about 17% under a magnetic field of 70 kOe at 5 K, which is much higher than that of the Fe_2CoSi compound and comparable to the MR in Fe_2TiSi films and the bulk spin-gapless semiconductor Mn_2CoAl [13,16,23].

Fig. 4(a) shows the Hall resistivity $\rho_{xy}(H)$ of the $Fe_2Ti_{0.5}Co_{0.5}Si$ Heusler compound measured between 5 K and 300 K. The $\rho_{xy}(H)$ curves have a sharp increase under low magnetic fields and become smooth with a small positive slope after the saturation of magnetization. The Hall resistivity ρ_{xy} can be expressed as $\rho_{xy}(H, T) = R_0 \cdot H + R_A \cdot M(H, T)$, where the first term depends on the external magnetic field (ordinary Hall resistivity) and the second term

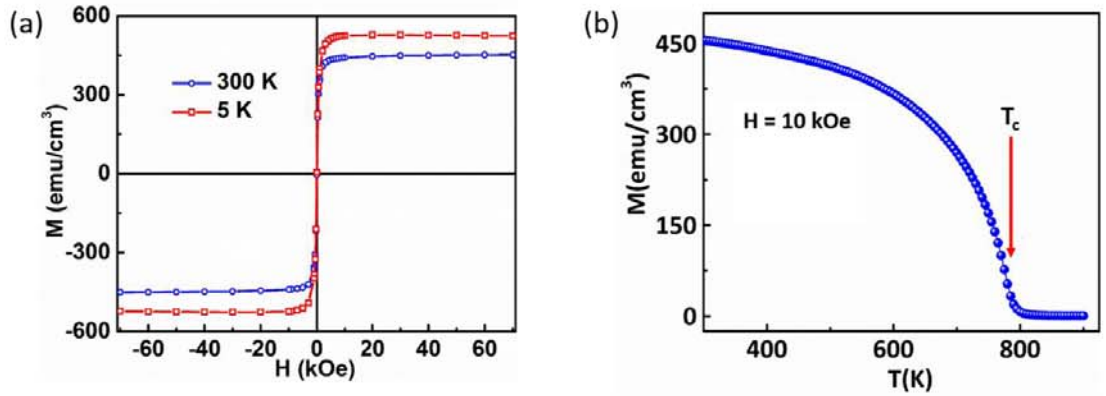

Fig. 2. (a) The magnetization M(H) of the $Fe_2Ti_{0.5}Co_{0.5}Si$ Heusler compound at 5 K and 300 K. (b) The temperature dependence of the magnetization of $Fe_2Ti_{0.5}Co_{0.5}Si$ at H = 10 kOe.

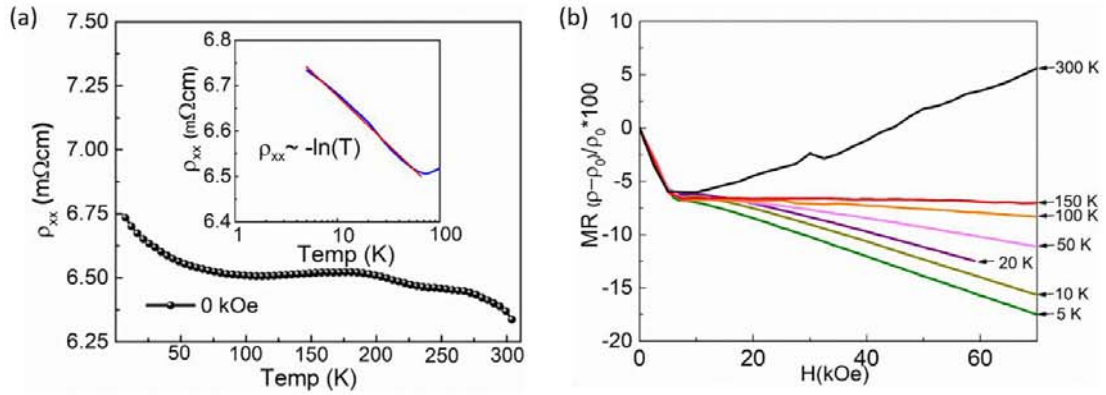

Fig. 3. (a) The longitudinal resistivity ρ_{xx} of $Fe_2Ti_{0.5}Co_{0.5}Si$ ribbons as a function of the temperature with no magnetic field applied. The inset shows the logarithmic temperature dependence of ρ_{xx} below 100 K. (b) Magnetoresistance of $Fe_2Ti_{0.5}Co_{0.5}Si$ at various temperatures.

depends on the magnetization of the film (anomalous Hall resistivity), with the coefficient R_0 in the expression being the ordinary Hall coefficient and R_A being the anomalous Hall coefficient [32]. These coefficients can be determined by extrapolating the high-field portion of $\rho_{xy}(H)$ curves to H = 0, where the slope and the intercept of a line are respectively equal to R_0 and R_AM_S, with M_S being the saturation magnetization. Accordingly, the carrier concentration n and the mobility μ in the compound are determined with the help of R_0 using the single-band model, i.e. $R_0 = 1/ne$ and $\mu = R_0(T)/\rho(T)$. Fig. 4(b) plots the carrier concentration n and the mobility μ as a function of the temperature (T), where the carrier concentration n may increase and the mobility μ decrease with the increasing temperature due to the thermal excitation of electrons, and increased phonon scattering, respectively. The values of the carrier concentration n and the mobility μ are

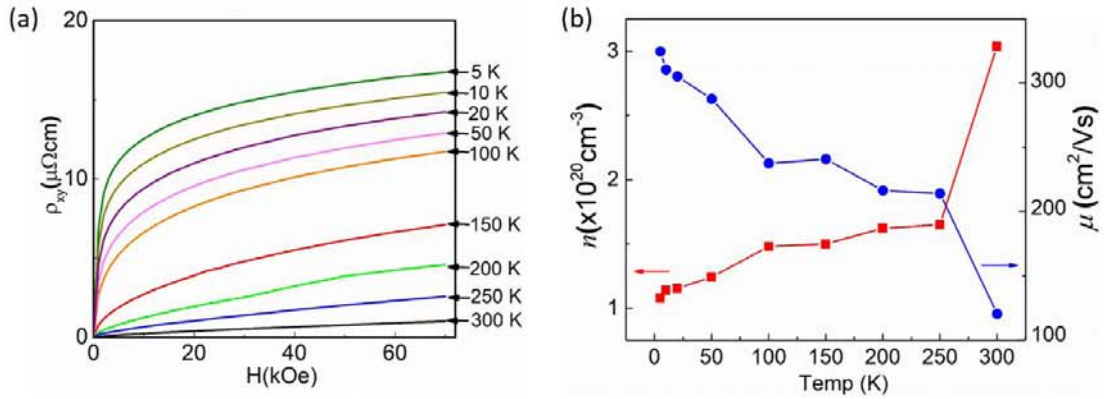

Fig. 4. (a) The Hall resistivity $\rho_{xy}(H)$ of $Fe_2Ti_{0.5}Co_{0.5}Si$ measured at various temperatures. (b) The temperature dependence of the carrier concentration n and the mobility μ of $Fe_2Ti_{0.5}Co_{0.5}Si$.

respectively $1.15 \times 10^{20}\,cm^{-3}$ and $315\,cm^2/(V{\cdot}s)$ at 5 K. The carrier concentration in $Fe_2Ti_{0.5}Co_{0.5}Si$ ribbons is lower than those in Fe_2TiSi thin films ($5.5 \times 10^{20}\,cm^{-3}$) [13], bulk Fe_2VAl ($10^{21}\,cm^{-3}$) [33] and spin-gapless semiconductor Mn_2CoAl films ($10^{22}\,cm^{-3}$) [22], but greater than those in HgCdTe (10^{15}–$10^{17}\,cm^{-3}$) [34] and bulk spin-gapless semiconductor Mn_2CoAl ($10^{17}\,cm^{-3}$) [23]. The carrier mobility in our samples is much higher than that in Fe_2TiSi thin films [13], CoFeCrAl films [30] and the Heusler spin-gapless semiconductor Mn_2CoAl [22,23], but comparable to the case of Si ($1.4 \times 10^3\,cm^2/(V{\cdot}s)$ for electrons and $4.5 \times 10^2\,cm^2/(V{\cdot}s)$ for holes) [35]. Although the weak temperature dependence of resistivity, the almost linear non-constant MR under high magnetic fields and the carrier concentration are similar to those of spin-gapless semiconductors, the variation in the temperature dependence of resistivity suggests an extrinsic semiconductor behavior. In general, the transport properties strongly suggest semiconducting behavior in the $Fe_2Ti_{0.5}Co_{0.5}Si$ compound.

4. Conclusions

In summary, the structural, magnetic and transport properties of the $Fe_2Ti_{0.5}Co_{0.5}Si$ Heusler compound are measured. The XRD analysis implies that the rapidly quenched $Fe_2Ti_{0.5}Co_{0.5}Si$ ribbons crystallize mainly in the $L2_1$ structure. This Heusler compound exhibits ferromagnetism, with the magnetization being 480 emu/cm^3 (2.36 μ_B/f.u.) at 5 K and a high Curie temperature of about 790 K. Transport measurements of $Fe_2Ti_{0.5}Co_{0.5}Si$ show semiconducting behavior with a negative temperature coefficient of resistivity. Interestingly, the substitution of half the Ti atoms in the paramagnetic semiconducting Fe_2TiSi Heusler compound with Co atoms results in a ferromagnetic Heusler compound with semiconducting behavior. These results are expected to stimulate further research on thin films of similar compositions and potential applications in spintronic devices.

Acknowledgements

This research was supported by United States, National Science Foundation (NSF), Division of Materials Research (DMR) under Award DMREF: SusChEM 1729288. The work was performed in part in the Nebraska Nanoscale Facility, Nebraska Center for Materials and Nanoscience, which is supported by the National Science Foundation under Award NNCI-1542182, and the Nebraska Research Initiative.

References

[1] C. Chappert, A. Fert, F.N. Van Dau, Nat. Mater. 6 (2007) 813–823.
[2] Z. Bai, L. Shen, G. Han, Y. Feng, SPIN 02 (2012) 1230006.
[3] Y. Ohno, D.K. Young, B. Beschoten, F. Matsukura, H. Ohno, D.D. Awschalom, Nature 402 (1999) 790–792.
[4] R.A. de Groot, F.M. Mueller, P.G.v. Engen, K.H.J. Buschow, Phys. Rev. Lett. 50 (1983) 2024–2027.
[5] R. Fiederling, M. Keim, G. Reuscher, W. Ossau, G. Schmidt, A. Waag, L.W. Molenkamp, Nature 402 (1999) 787–790.
[6] T. Dietl, H. Ohno, Rev. Mod. Phys. 86 (2014) 187–251.
[7] T. Graf, C. Felser, S.S.P. Parkin, Prog. Solid State Chem. 39 (2011) 1–50.
[8] F. Casper, T. Graf, S. Chadov, B. Balke, C. Felser, Semicond. Sci. Technol. 27 (2012) 063001.
[9] K. Bartholomé, B. Balke, D. Zuckermann, M. Köhne, M. Müller, K. Tarantik, J. König, J. Electron. Mater. 43 (2014) 1775–1781.
[10] D.I. Bilc, G. Hautier, D. Waroquiers, G.-M. Rignanese, P. Ghosez, Phys. Rev. Lett. 114 (2015) 136601.
[11] Y. Shin, O. Masakuni, N. Akinori, K. Yosuke, H. Jun, Appl. Phys. Exp. 6 (2013) 025504.
[12] I. Galanakis, P.H. Dederichs, N. Papanikolaou, Phys. Rev. B 66 (2002) 174429.
[13] M. Meinert, M.P. Geisler, J. Schmalhorst, U. Heinzmann, E. Arenholz, W. Hetaba, M. Stöger-Pollach, A. Hütten, G. Reiss, Phys. Rev. B 90 (2014) 085127.
[14] A. Ślebarski, M.B. Maple, E.J. Freeman, C. Sirvent, D. Tworuszka, M. Orzechowska, A. Wrona, A. Jezierski, S. Chiuzbaian, M. Neumann, Phys. Rev. B 62 (2000) 3296–3299.
[15] S.V. Dordevic, D.N. Basov, A. Ślebarski, M.B. Maple, L. Degiorgi, Phys. Rev. B 66 (2002) 075122.
[16] Y. Du, G.Z. Xu, X.M. Zhang, Z.Y. Liu, S.Y. Yu, E.K. Liu, W.H. Wang, G.H. Wu, EPL 103 (2013) 37011.
[17] X. Wang, Z. Cheng, H. Yuan, R. Khenata, J. Mater. Chem. C 5 (2017) 11559.
[18] Y. Nishino, S. Deguchi, U. Mizutani, Phys. Rev. B 74 (2006) 115115.
[19] Y. Nishino, M. Kato, S. Asano, K. Soda, M. Hayasaki, U. Mizutani, Phys. Rev. Lett. 79 (1997) 1909–1912.
[20] H. Okamura, J. Kawahara, T. Nanba, S. Kimura, K. Soda, U. Mizutani, Y. Nishino, M. Kato, I. Shimoyama, H. Miura, K. Fukui, K. Nakagawa, H. Nakagawa, T. Kinoshita, Phys. Rev. Lett. 84 (2000) 3674–3677.
[21] Y. Jin, J. Waybright, P. Kharel, I. Tutic, J. Herran, P. Lukashev, S. Valloppilly, D.J. Sellmyer, AIP Adv. 7 (2017) 055812.
[22] M.E. Jamer, B.A. Assaf, T. Devakul, D. Heiman, Appl. Phys. Lett. 103 (2013) 142403.
[23] S. Ouardi, G.H. Fecher, C. Felser, J. Kübler, Phys. Rev. Lett. 110 (2013) 100401.
[24] L. Bainsla, A.I. Mallick, M.M. Raja, A.K. Nigam, B.S.D.Ch.S. Varaprasad, Y.K. Takahashi, A. Alam, K.G. Suresh, K. Hono, Phys. Rev. B 91 (2015) 104408.
[25] H. Fu, Y. Li, L. Ma, C. You, Q. Zhang, N. Tian, J. Magn. Magn. Mater. 473 (2019) 16.
[26] A.K. Dasadia, B.B. Nariya, A.R. Jani, Optoelectron. Adv. Mat. 7 (2013) 70.
[27] J. Kondo, Progr. Theor. Exp. Phys 32 (1964) 37–49.
[28] N. Giordano, Phys. Rev. B 53 (1996) 2487–2491.
[29] J. Schoenes, C. Schönenberger, J.J.M. Franse, A.A. Menovsky, Phys. Rev. B 35 (1987) 5375–5378.
[30] P. Kharel, R. Skomski, P. Lukashev, R. Sabirianov, D.J. Sellmyer, Phys. Rev. B 84 (2011) 014431.
[31] Y. Jin, P. Kharel, S.R. Valloppilly, X.-Z. Li, D.R. Kim, G.J. Zhao, T.Y. Chen, R. Choudhary, A. Kashyap, R. Skomski, D.J. Sellmyer, Appl. Phys. Lett. 109 (2016) 142410.
[32] N. Nagaosa, J. Sinova, S. Onoda, A.H. MacDonald, N.P. Ong, Rev. Mod. Phys. 82 (2010) 1539–1592.
[33] V.I. Okulov, V.E. Arkhipov, T.E. Govorkova, A.V. Korolev, K.A. Okulova, E.I. Shreder, V.V. Marchenkov, H.W. Weber, Low Temp. Phys. 33 (2007) 692–698.
[34] I.M. Tsidilkovski, Springer Series in Solid-State Sciences, vol. 116, 1996.
[35] See the electronic archive New Semiconductor Materials maintained at the Ioffe Institute: http://www.ioffe.rssi.ru/SVA/NSM/Semicond/i.